eISSN 2005-5447
International Journal of Stem Cells Vol. 16, No. 4, 2023 https://doi.org/10.15283/ijsc23036

ORIGINAL ARTICLE

Differentiation and Characterization of Cystic Fibrosis Transmembrane Conductance Regulator Knockout Human Pluripotent Stem Cells into Salivary Gland Epithelial Progenitors

Shuang Yan[1], Yifei Zhang[1], Siqi Zhang[1], Shicheng Wei[1,2]

[1]*Department of Oral and Maxillofacial Surgery, School and Hospital of Stomatology and Central Laboratory, Peking University, Beijing, China*
[2]*Institute of Molecular Medicine, Peking University, Beijing, China*

The differentiation of pluripotent stem cells has been used to study disease mechanisms and development. We previously described a method for differentiating human pluripotent stem cells (hPSCs) into salivary gland epithelial progenitors (SGEPs). Here, cystic fibrosis transmembrane conductance regulator (CFTR) knockout hPSCs were differentiated into SGEPs derived from CFTR knockout hESCs (CF-SGEPs) using the same protocol to investigate whether the hPSC-derived SGEPs can model the characteristics of CF. CF—a disease that affects salivary gland (SG) function—is caused by mutations of the *CFTR* gene. Firstly, we successfully generated CFTR knockout hPSCs with reduced CFTR protein expression using the CRISPR-Cas9 system. After 16 days of differentiation, the protein expression of CFTR decreased in SGEPs derived from CFTR knockout hESCs (CF-SGEPs). RNA-Seq revealed that multiple genes modulating SG development and function were down-regulated, and positive regulators of inflammation were up-regulated in CF-SGEPs, correlating with the salivary phenotype of CF patients. These results demonstrated that CFTR suppression disrupted the differentiation of hPSC-derived SGEPs, which modeled the SG development of CF patients. In summary, this study not only proved that the hPSC-derived SGEPs could serve as manipulable and readily accessible cell models for the study of SG developmental diseases but also opened up new avenues for the study of the CF mechanism.

Keywords: Cystic fibrosis, Salivary gland, Human embryonic stem cells, Progenitors, Cystic fibrosis transmembrane conductance regulator

Received: March 24, 2023, Revised: May 15, 2023,
Accepted: June 24, 2023, Published online: September 6, 2023
Correspondence to **Shicheng Wei**
Department of Oral and Maxillofacial Surgery, School and Hospital of Stomatology and Central Laboratory, Peking University, 5 Yiheyuan Rd, Haidian District, Beijing 100871, China
E-mail: sc-wei@pku.edu.cn
Co-Correspondence to **Siqi Zhang**
Department of Oral and Maxillofacial Surgery, School and Hospital of Stomatology and Central Laboratory, Peking University, 5 Yiheyuan Rd, Haidian District, Beijing 100871, China
E-mail: 18612769160@163.com

Introduction

Pluripotent stem cells (PSCs) can self-renewal and differentiate into all cell types derived from the three germ layers (1). Therefore, PSCs have demonstrated promising application prospects in regenerative medicine, developmental biology, and disease modeling (2). They have been applied to multiple human organs, including the brain, heart, stomach, intestine, bone, pancreas, and liver (3-9).

Salivary glands (SGs) are vital organs in the oral cavity, primarily composing of the parotid, submandibular, sublingual, and many small glands (10). The primary function of SGs is to secrete saliva. Saliva has the functions of lubricating the mouth, aiding digestion, promoting den-

tal health, and maintaining oral homeostasis (11). Few studies have been conducted on inducing the differentiation of PSCs into SGs (12, 13). Our group previously established a protocol for differentiating human embryonic stem cells (hESCs) into salivary gland epithelial progenitors (SGEPs), which recapitulated the characteristics of developing human SGs (13). However, it is still unknown whether the differentiation of SGEPs can be further applied to the study of SG development-related diseases.

Cystic fibrosis (CF) is the most common autosomal recessive genetic disease associated with exocrine gland dysfunction. It is caused by mutations in the cystic fibrosis transmembrane conductance regulator (*CFTR*) gene, resulting in non-expression or reduced expression of the CFTR protein (14). The most common CFTR mutation is the deletion of a single phenylalanine residue at position 508 in the CFTR protein, known as the ⊿F508 mutation. This mutation has deleterious effects on the processing of CFTR protein within the endoplasmic reticulum, resulting in a dramatic decrease in protein levels expressed on the plasma membrane of epithelial cells, with unchanged CFTR mRNA expression levels (15, 16). SG involvement is a common symptom of CF disease. An epidemiological survey found that 92% of CF children had enlarged submandibular glands. Chronic swelling of the submandibular glands is one of the common clinical manifestations in CF children (17). CF patients also exhibit clinical manifestations of the decreased saliva flow rate, hyposalivation, an increased caries rate, and blockage of ducts and acini (18, 19). Notably, the CFTR-knockout mouse model lacked granular ducts in the SGs (20). In this study, we used the CRISPR-Cas9 system to construct CFTR-knockout hESCs and explored whether our previously reported SGEPs could model the characteristics of CF.

We first successfully generated a CFTR knockout hESCs and confirmed a decrease in CFTR protein expression. After 16 days of differentiation, CFTR protein expression also decreased in SGEPs derived from CFTR knockout hESCs (CF-SGEPs). Furthermore, RNA-Seq revealed a low expression of multiple SG development-related genes in CF-SGEPs and reduced expression of genes involved in saliva secretion. The expression of positively regulated inflammation genes increased. These results confirmed that the CF-SGEPs mimic the development of SGs in CF patients.

Materials and Methods

Cell culture and SGEPs differentiation

The hESC lines H1 were kindly provided by WiCell Research Institute. The hESC lines H1 (H1ES) were maintained under feeder-free conditions and passaged on Matrigel^{TM} (1 : 160 dilution) coated plates in mTeSR^{TM} medium (STEMCELL Technologies) supplemented with 1% penicillin/streptomycin. At 70%～80% confluence, H1 cells were passaged by 5-minute incubation with ethylenediaminetetraacetic acid. The cells were then dissociated by gently blowing 3 times with a pipette and plated into a six-well plate coated with Matrigel (1 : 160 dilution) in mTeSR^{TM} medium. The differentiation of SGEPs was performed as previously described (13). H1 cells were digested with Dispase II for 5-minute and the cell aggregates were suspended in low-adhesion culture plates for three days to form embryoid bodies (EBs). The differentiation medium was DMEM/F12 medium with 10% knockout serum replacement, 1.5% FBS, 1 mM GlutaMAX, 2 mM NEAA, 1 mM penicillin-streptomycin and 0.14 mM 2-mercaptoethanol. EBs were transferred to a six-well plate at a ratio of 1 : 3 to allow cell adherence for 2 additional days. Then, cells were cultured in differentiation medium plus 10 pM BMP4 from day 5 to day 10. RA was applied to the cultures on day 10 for 2 days at a final concentration of 1 μM, followed by a 4-day treatment of 6 μM CHIR99021 to induce SGEP specification. The fresh medium was changed every 2 days.

CRISPR-Cas9 genomic editing

The construction of the single-guide RNA (sgRNA) expression vector was performed as previously described (21). Briefly, the *CFTR* gene sequence was searched on GenBank and then *CFTR* (gene number NC_000007.14) sequence was analyzed. Based on the ninth exon sequence, oligos for guide RNAs were selected with the help of the online platform chopchop and 5'-CACCG-3' was added to the five prime end of the oligo (5'-CACCG tctgtatctatattcatcat-3', 5'- AAACatgatgaatatagatacagaC-3'). Annealed guide oligos were cloned into the CRISPR-Cas9 expression vector pSpCas9(BB)-2A-puro (PX462) (#48141, Addgene plasmid). The vector was linearized with BbsI (Thermo Fisher Scientific), and guide oligos were cloned into the vector with T4 DNA ligase (cat#15224041, Invitrogen). The recombination plasmid was expanded with trans5 alpha-competent cells and extracted with the plasmids extraction kit according to the manufacturer's instructions.

At 70%～80% confluence, the H1 cells were transfected with 2 μg of PX462 plasmid and 8 μl of Lipofectamine 3000 per well. After 24 hours, the cells were treated with Accutase (Gibco) to obtain a single cell suspension. The cells were then resuspended and plated into a six-well plate coated with Matrigel in mTesR1 containing 10 μM Y27632 and 0.75 μg/ml of puromycin. Puromycin was removed af-

ter 48 hours, and the cells were maintained in mTesR1 for 10～14 days until colonies were large enough to be isolated. The cell pellet was collected under a microscope and inoculated into a 24-well plate to continue the culture.

DNA extraction and sequencing

The cells were cultured in 6-well plates, and the genomic DNA was isolated using the Agencourt DNAdvance Genomic DNA Isolation Kit (TIANGEN) according to the manufacturer's instructions. On-target genomic regions of interest were amplified using PrimeSTAR HS DNA Polymerase (Takara) and primers (Supplementary Table S1). The polymerase chain reaction (PCR) products were used to perform sanger sequencing (NovaSeq 6000; Illumina).

Western blot

The cells were lysed with RIPA regent, and the supernatant was centrifuged to obtain the sample. The concentration of total proteins was measured using the BCA Kit (Solarbio). Samples were electrophoresed on sodium dodecyl sulfate-polyacrylamide gel electrophoresis at 60 V for 60 minutes. After being transferred to the polyvinylidene difluoride (PVDF) membrane with 300 mA for 180 minutes, the PVDF membrane was blocked in tris-buffered saline-0.05% Tween-20 with 5% non-fat milk at 37℃ for 60 minutes and then incubated overnight at 37℃ with primary antibodies. The PVDF membrane was then incubated with secondary antibodies after extensive wash. After three washes, immunoblots were visualized using ECL Western Blotting Detection System (Bio-Rad). The primary and secondary antibodies are rabbit anti-β actin (Solarbio), mouse anti-CFTR (Santa Cruz), goat anti-mouse IgG-HRP (Absin) and goat anti-rabbit IgG-HRP (Absin).

Off-target analysis

Off-target sites prediction of selected sgRNA was performed using the online CRISPR-Cas9 Design tool (https://chopchop.cbu.uib.no/). A 500-bp region was amplified using PCR with PrimeSTAR® Max DNA Polymerase (Takara), and forward and reverse primers for each gene are reported in Supplementary Table S1. Amplification was performed as follows: 30 cycles consisting of 98℃ for 10 seconds, 55℃ for 5 seconds, and 72℃ for 10 seconds. PCR products were purified and sequenced using Sanger methods.

Immunofluorescence

Seeded cells on glass bottom dishes were fixed with 4% paraformaldehyde for 30 minutes at room temperature or overnight at 4℃. The cells were treated with 0.1% Triton X-100 at room temperature for 10 minutes, and then blocked in 3% BCA for 2 hours at room temperature. The samples were incubated with primary antibodies in the blocking buffer overnight at 4℃ and incubated with secondary antibodies for 1 hour at room temperature. Finally, the cells were stained with DAPI (1 μg/ml) and observed using a A1R-si confocal microscope (Nikon).

RNA extraction and quantitative real-time polymerase chain reaction

Total RNA was extracted using the FastPure® Cell/Tissue Total RNA Isolation Kit (Vazyme). cDNA synthesis was performed using HiScript® II Q Select RT SuperMix for quantitative real-time polymerase chain reaction (qPCR) (+gDNA wiper) (Vazyme), according to the manufacturer's instructions. The mRNA expression levels were measured using qPCR with SYBR Green master mix (Roche) as follows: predenaturation at 95℃ for 10 minutes, followed by the introduction of 40 cycles of 95℃ for 5 seconds and 60℃ for 30 seconds. The qPCR primers are presented in Supplementary Table S2.

RNA sequencing and analysis

On day 16, total RNA was extracted from wild type (WT) and CF-SGEPs with the FastPure® Cell/Tissue Total RNA Isolation Kit, according to the manufacturer's instructions. RNA concentration and quality were measured using NanoDrop 2000 (Thermo Fisher Scientific) and the 2100 Bioanalyzer system (Agilent Technologies). According to the manufacturer's recommendation, sequencing libraries were prepared using NEBNext Ultra™ RNA Library Prep Kit for Illumina (New England Biolabs). The index codes were added to the attribute sequences of each sample. Sequencing was performed on Novaseq 6000 platform, and paired-end reads were generated. Quality-controlled clean data was generated and then mapped to the reference genome (GRCh38_release95) using Hisat2. Quantification of gene expression levels was measured using fragments per kilobase of transcript per million fragments mapped. DESeq2 was used to perform differential expression analysis and genes with an adjusted p-value＜0.01 were considered as differentially expressed.

Statistical analysis

The data are presented as mean±SD deviation of three independent experiments. Statistical significance was calculated with a two-tailed, unpaired Student's t-test. Multiple group comparisons were performed using one-way ANOVA followed by Tukey's multiple comparison test. Significant difference was tested at $p<0.05$, $p<0.01$, and $p<0.001$.

Results

Construction of hESCs clones with CFTR mutation

To generate a hESC line with *CFTR* gene mutation, we first used the CRISPR-Cas9 system to interrupt the *CFTR* gene. As the most common mutation of CFTR is the ⊿F508 on the ninth exon, we used the online CRISPR design tool chopchop to design a sgRNA around the ⊿F508 (Fig. 1A). The sgRNA expression construct was prepared using the CRISPR-Cas9 expression vector PX462. Guide oligos were successfully cloned into CRISPR-Cas9 expression vectors after sanger sequencing (Supplementary Fig. S1A). Recombinant plasmids were then transfected into hESCs. After a screening, 30 clones were selected. After Sanger sequencing, one of the clones had a mutation in the *CFTR* gene, which was called a CFTR knockout hESCs. Sanger sequencing revealed that the CFTR knockout hESCs had an adenine deoxynucleotide inserted compared with the WT cell line (Fig. 1B). Furthermore, the sequence analysis of the off-targets cleavage sites, based on the used sgRNA, revealed no alterations in the investigated genomic regions, indicating the absence of undesired genome modifications mediated by the Cas9 protein (Supplementary Table S3). Moreover, CFTR knockout hESCs showed no changes in mRNA levels and reduced protein expression levels of CFTR in comparison to WT cells (Fig. 1C, 1D, Supplementary Fig. S1B), which were similar to those of ⊿F508 (15).

Pluripotency of *CFTR* gene mutant hESCs clones

Before induction into SGEPs, we must ensure that the gene editing process has no effect on the pluripotency of CFTR knockout hESCs. The CFTR knockout hESCs presented normal morphology (Fig. 2A). We also examined the expression of *OCT4*, *NANOG*, *SOX2*, and *KLF4*, pluripotent markers of hESCs. The expression levels of *OCT4*,

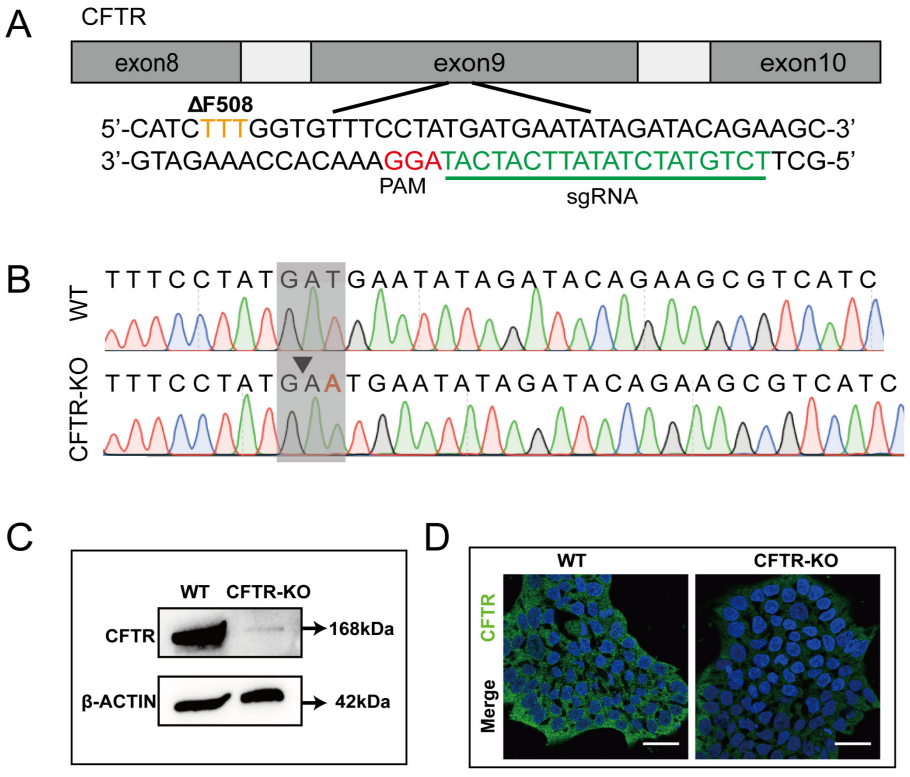

Fig. 1. Construction of a mutant cystic fibrosis transmembrane conductance regulator (*CFTR*) gene hESCs clone. (A) Schematic diagram of the CRISPR/Cas9 guide RNA (gRNA) targeting exon9 of the *CFTR* gene: three exons of *CFTR* gene are shown, with the gRNA targeting a specific region of exon 9, orange sequence represents the position of the ⊿F508 mutation, red sequences represent protospacer adjacent motif (PAM), and green sequences with underscore represent single-guide RNA (sgRNA). (B) Electropherograms comparison between the wild-type cells and CFTR knockout human embryonic stem cells (hESCs). A insertion of 1 bp was detected using Sanger sequencing in CFTR knockout hESCs. The black triangle indicates the predicted cut site of the Cas9 nuclease. The gray boxes highlight sequences that differ between CFTR knockout hESCs and the wild type. (C) Western blot. β-Actin was used as a loading control. CFTR protein expression levels were assessed by Western blot analysis. (D) Immunofluorescence staining revealed that the wild type and CFTR knockout hESCs expressed CFTR. Scale bar=20 μm. WT: the wild-type hESCs, CFTR-KO: CFTR knockout hESCs.

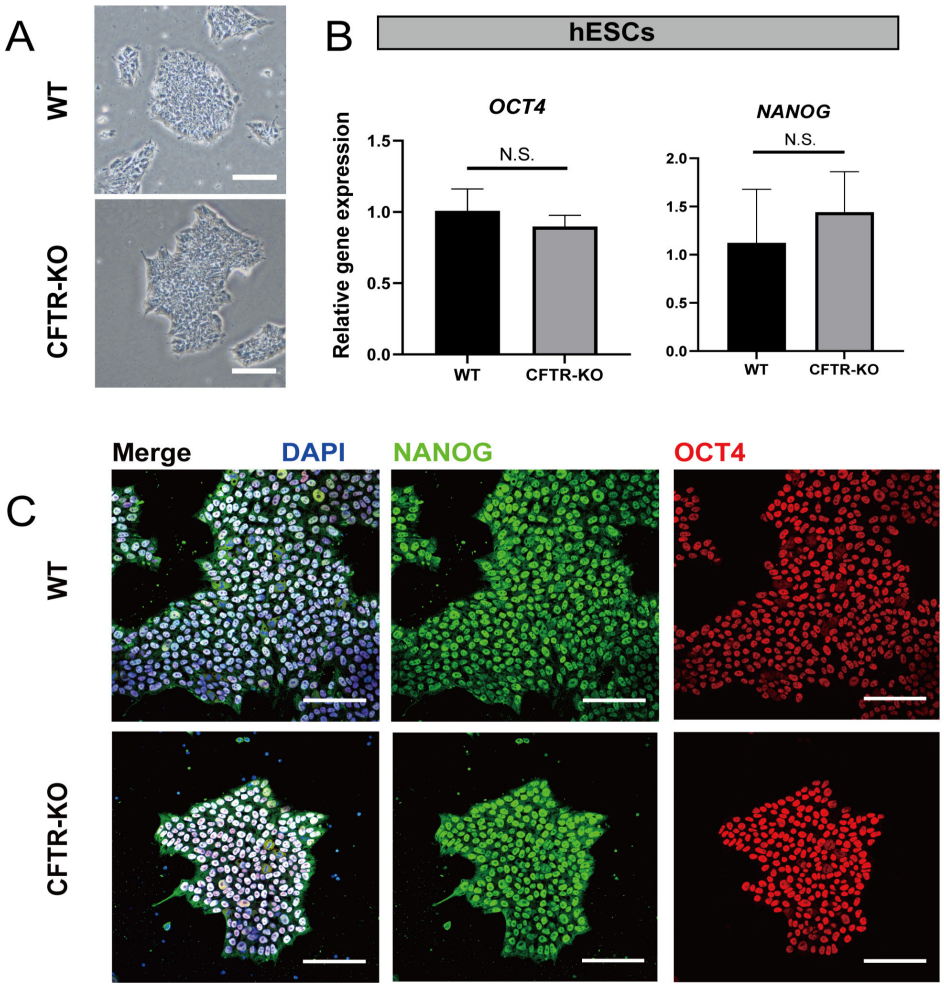

Fig. 2. Pluripotency detection of cystic fibrosis transmembrane conductance regulator (CFTR) knockout human embryonic stem cells (hESCs) and the wild-type hESCs. (A) Bright-field images showed the morphology of the wild-type cells and CFTR knockout hESCs. Scale bar=200 μm. (B) *OCT4* and *NANOG* expression levels of wild type and CFTR knockout hESCs were detected. Data are presented as mean±SD and were normalized to β-actin in three independent experiments. The results were reported as the fold change compared to the wild-type hESCs by unpaired, two-tailed Student's t-test. (C) Immunofluorescence staining showed that the wild-type hESCs and CFTR knockout hESCs expressed OCT4 and NANOG. Scale bar=75 μm. WT: the wild-type hESCs, CFTR-KO: CFTR knockout hESCs, N.S.: no significant.

NANOG, *SOX2*, and *KLF4* in CFTR knockout hESCs were comparable to the WT (Fig. 2B, Supplementary Fig. S1C). Immunofluorescence analysis also revealed the similar results for two cells (Fig. 2C). Previous studies have demonstrated that the expression of target genes of the Wnt pathway is decreased in murine embryonic stem cells that do not express the CFTR protein (22). To investigate whether the same observations were present in hESCs, we examined the expression of Wnt pathway target genes—*AXIN2*, *CD44*, *CCND1*, and *CCND2*. However, there was no significant difference in the expression of AXIN2, CD44, CCND1, and CCND2 between CFTR knockout hESCs and WT (Supplementary Fig. S2A), which may be due to species-specific differences between humans and mice. Overall, the aforementioned data suggested that the pluripotency of CFTR knockout hESCs was maintained.

Differentiation of CFTR knockout hESCs into SGEPs

The CFTR knockout hESCs were induced into SGEPs. First of all, hESCs were cultured in suspension to form EBs for three days. (Fig. 3A). During the suspension culture of EBs, the number of EBs had decreased in CFTR knockout hPSCs cultures under the same conditions (Fig. 3B). On the third day of differentiation, EBs derived from CFTR knockout hESCs exhibited decreased ectoderm (*PAX6*) expression, increased mesoderm (*T*) expression, and no difference in the endoderm (*GATA4*) expression compared with WT EBs (Fig. 3C). The expression levels of Wnt pathway target genes—*AXIN2*, *CD44*, and *CCND2*—did not differ between EBs differentiated from CFTR knockout hESCs and the WT EBs (Supplementary Fig. S2B).Compared with the WT EBs, the expression levels of Wnt pathway target gene *CCND1* in EBs differentiated from CFTR knockout hESCs was decreased (Supplementary Fig. S2B). These data revealed that CFTR knockout might affect the Wnt pathway.

According to the protocol described previously (13), the CFTR knockout hESCs were induced to differentiate for

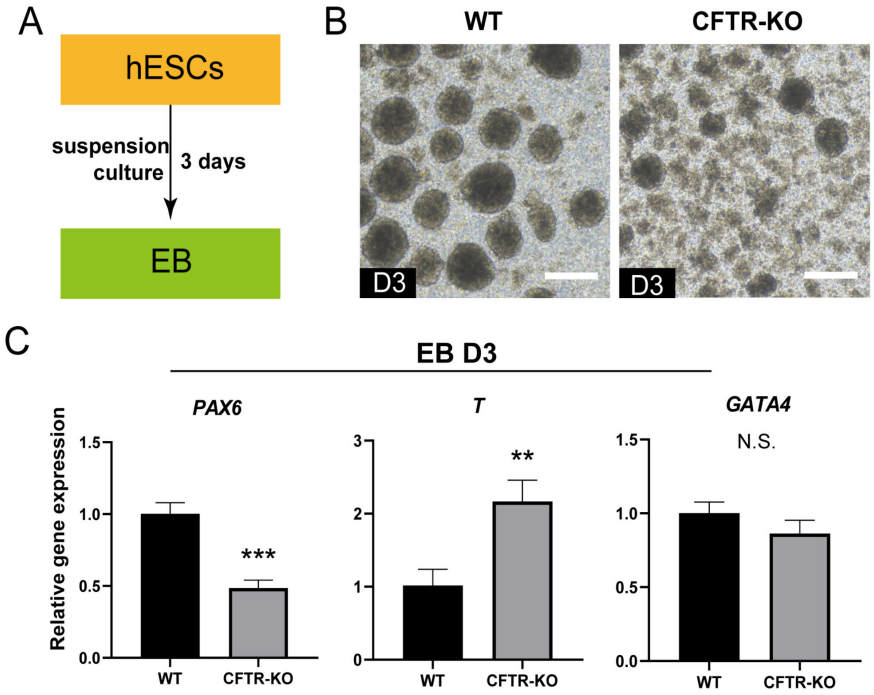

Fig. 3. Formation of cystic fibrosis transmembrane conductance regulator (CFTR) knockout and wild type human embryonic stem cells (hESCs) to embryoid bodies (EBs). (A) EBs were formed in suspension culture condition for 3 days. (B) Brightfield images showed the morphology of EBs from CFTR knockout and wild-type hESCs on the third day of suspension culture. Scale bar=200 μm. (C) The expressions of three germ layer markers were examined on day 3. The data are presented as mean±SD, and were normalized to β-actin in three independent experiments. The results were reported as the fold change compared to the wild-type hESCs by unpaired, two-tailed Student's t-test; **p<0.01 and ***p<0.001. WT: EBs derived from the wild-type hESCs, CFTR-KO: EBs derived from CFTR knockout hESCs, N.S.: no significant.

16 days to form CF-SGEPs by adding BMP4, RA, and CHIR99021 to the differentiation medium successively (Fig. 4A). After the 16 days of the differentiation, there was no difference in the morphology of CF-SGEPs, which was similar to that described in the previously described (Fig. 4B) (13). CFTR mRNA levels of CF-SGEPs were similar to WT (Fig. 4C). The Western blot and immunofluorescence staining results revealed that the protein expression of CFTR in CF-SGEPs was decreased (Fig. 4D, 4E). It is worth mentioning that the mRNA level of CFTR in the cells of patients with the ΔF508 mutation is similar to that of normal individuals, and the expression of mature CFTR protein is decreased (16). Therefore, these results suggested that the CF-SGEPs mimicked the gene expression characteristics of CF patients. On day 16, we then examined the Wnt target genes of SGEPs. The expression of *LEF1*, *CD44*, *CCND1*, and *CCND2* was decreased, and there was no difference in *AXIN2* (Fig. 4F, 4G). These data indicated that CFTR protein may affect the Wnt pathway, while we successfully constructed SGEPs with robust correlations to CF features.

RNA-Seq reveals gene expression differences between CF-SGEPs and the SGEPs derived from the WT hESCs

To further demonstrate that the CF-SGEPs could model the characteristics of CF patients, we performed a transcriptome analysis of CF-SGEPs. The results of hierarchical cluster analysis of differentially expressed genes between SGEPs derived from the WT hESCs (WT-SGEPs) and CF-SGEPs revealed that the gene expression of CF-SGEPs was quite different from that of the WT (Fig. 5A). Differences between the transcriptome sequencing data of WT-SGEPs and CF-SGEPs were analyzed and statistical histogram (Supplementary Fig. S3A) and volcano map (Supplementary Fig. S3B) were drawn. Among the differential genes, 593 genes were up-regulated, 1,348 genes were down-regulated, and the number of down-regulated genes was relatively large, accounting for 69% of the total (Supplementary Fig. S3). We conducted Gene Ontology (GO) analysis to investigate the difference between CF-SGEPs and WT-SGEPs (Fig. 5B). The significant GO terms of genes with low expression in CF-SGEPs were related to SG development including tube development, positive regulation of cell differentiation, and morphogenesis of an

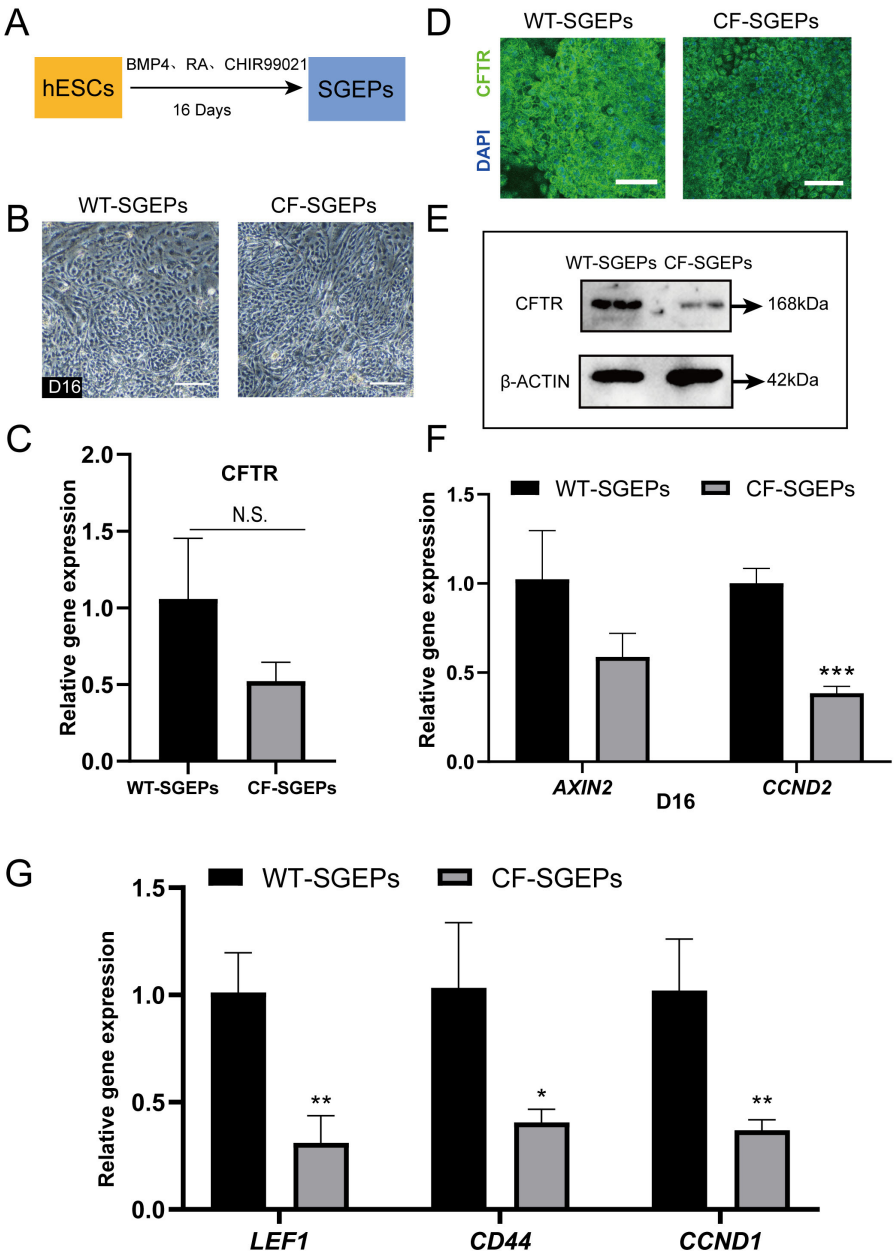

Fig. 4. Formation of salivary gland epithelial progenitors (SGEPs) by induction of H1ES differentiation. (A) The protocol of derivation of SGEPs from human embryonic stem cells (hESCs) by BMP4, RA, and CHIR99021. (B) Brightfield images showed the morphology of SGEPs from cystic fibrosis transmembrane conductance regulator (CFTR) knockout hESCs and wild-type hESCs on day 16. Scale bar=200 μm. (C) Real-time polymerase chain reaction (PCR) analysis of CFTR in SGEPs on day 16. Data are presented as mean±SD and were normalized to β-actin in three independent experiments. The results are reported as the fold change compared to the wild type SGEPs by unpaired, two-tailed Student's t-test. (D) Immunofluorescence staining showed that SGEPs from H1ES wild-type cells and clone 28 expressed CFTR. Scale bar=75 μm. (E) Western blot. β-actin was used as a loading control. CFTR protein expression levels of SGEPs were assessed by Western blot analysis. (F) Real-time PCR analysis of Wnt downstream targets *AXIN2* and *CCND2* in SGEPs on day 16. Data are presented as mean±SD and were normalized to β-actin in three independent experiments. The results are reported as the fold change compared to the wild-type SGEPs by unpaired, two-tailed Student's t-test; ***p<0.001. (G) Real-time PCR analysis of Wnt downstream targets *LEF1*, *CD44*, and *CCND1* in SGEPs on day 16. Data are presented as mean±SD and were normalized to β-actin in three independent experiments. The results are reported as the fold change compared to the wild-type SGEPs by unpaired, two-tailed Student's t-test; *p<0.05 and **p<0.01. WT-SGEPs: SGEPs derived from the wild-type hESCs, CF-SGEPs: SGEPs derived from CFTR knockout hESCs, N.S.: no significant.

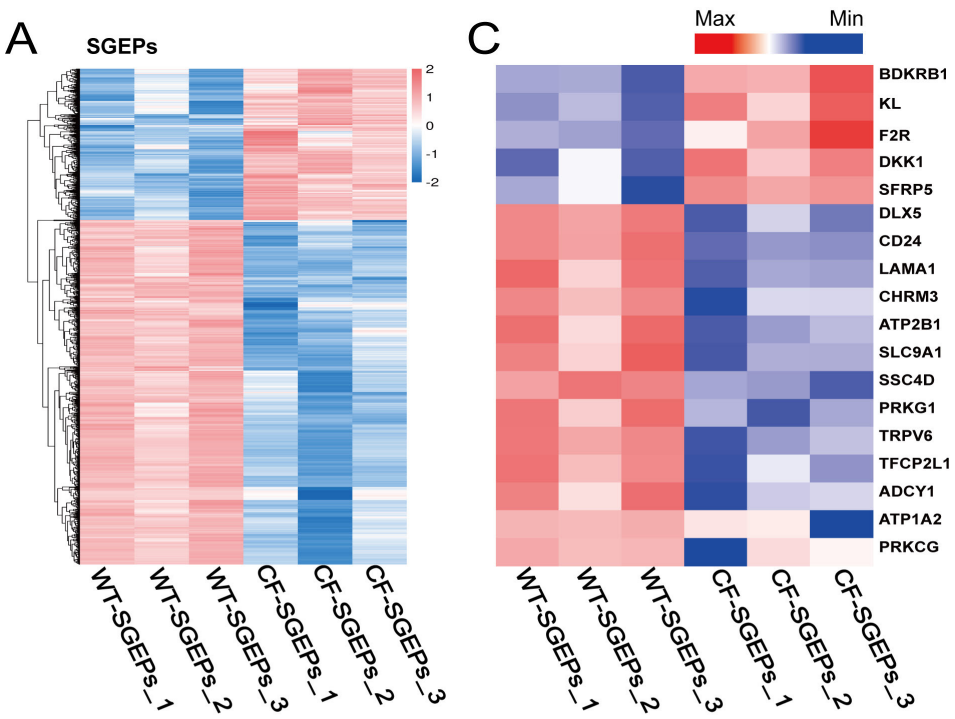

B

Significant GO terms

tube development	p=0.00181
positive regulation of cell differentiation	P=0.00241
morphogenesis of an epithelial sheet	P=0.00416
canonical Wnt signaling pathway	P=0.00827
regulation of canonical Wnt signaling pathway	P=0.01409
Wnt signaling pathway	P=0.02774
regulation of lipid metabolic process	P=0.00023
transport	p=0.00869
sodium ion transport	p=0.0166
positive regulation of transport	p=0.03196

Fig. 5. Salivary gland epithelial progenitors (SGEPs) had different gene expression profiles between the wild type SGEPs and CF-SGEPs. (A) A SGEPs' hierarchical cluster analysis of differentially expressed genes between the wild type SGEPs and CF-SGEPs. False Discovery Rate<0.01, fold change≥2. (B) Significant Gene Ontology (GO) terms (biological processes) for differentially expressed genes were represented. (C) A heatmap revealed expression profiles of essential genes related to the human salivary gland canonical Wnt pathway, inflammation, development, maturation, and secretion. WT-SGEPs: SGEPs derived from the wild-type human embryonic stem cells, CF-SGEPs: SGEPs derived from cystic fibrosis transmembrane conductance regulator knockout human embryonic stem cells, Max: maximum, Min: minimum.

epithelium sheet. Compared with WT-SGEPs, the other significant GO terms of with low expression in CF-SGEPs was related to transport and canonical Wnt signaling pathway (Fig. 5B). The heat map revealed the expression of the SG progenitor cell marker CD24 (23), the key gene of SG development LAMA1 (24, 25), and the marker of SG maturation CHRM3 were decreased in the CF-SGEPs (Fig. 5C). The qPCR data also revealed the same tendency (Fig. 6A). Notably, we found that the CF-SGEPs exhibited decreased expression of multiple salivary secretion-related markers such as ATP2B1, SLC9A1, PRKG1, SSC4D, and TRPV6. (Fig. 5C, 6B). These results were similar to the salivation deficits seen in CF patients. The expression of inflammatory molecules in CF patients is elevated (26). Interestingly, the expression of positive regulatory genes for inflammation, including BDKRB1, F2R, and KL, was increased (Fig. 5C). The qPCR data revealed that the mRNA level of KL was not significantly changed in CF-SGEPs, and the mRNA level of BDKRB1 and F2R in CF-SGEPs was increased (Fig. 6C). Thus, these data revealed that there was a strong association between CF-SGEP and CF phenotypes. Furthermore, compared with the WT, the expression of the negative regulatory genes—*DKK1* and *SFRP5*—of the canonical Wnt pathway of the CF-SGEPs was increased, and the expression of the positive regulatory gene *DLX5* was decreased (Fig. 5C). The

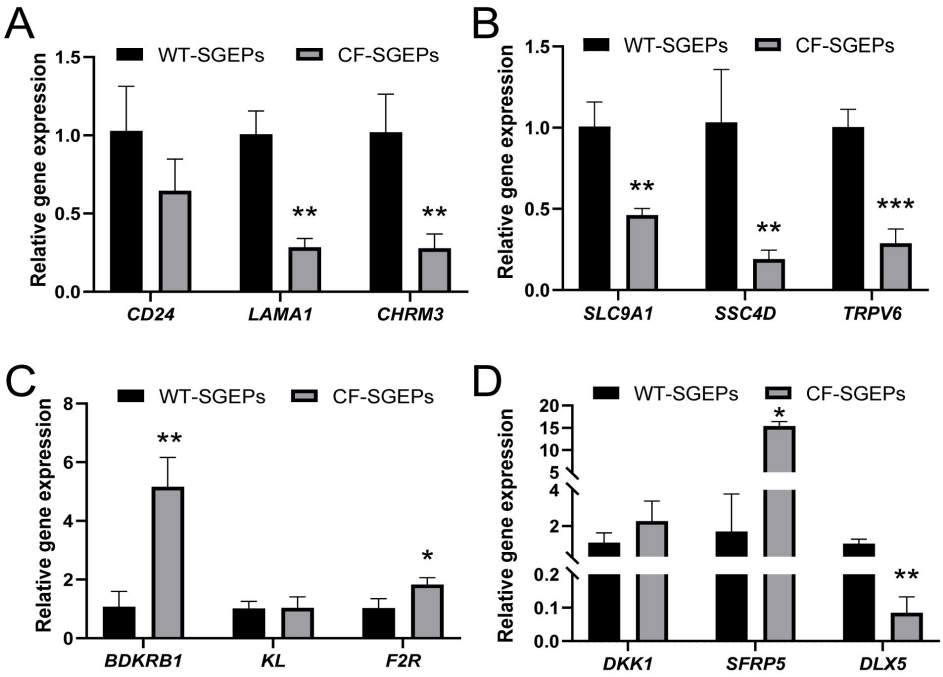

Fig. 6. Real-time polymerase chain reaction (PCR) analysis of salivary gland epithelial progenitors (SGEPs) on day 16 quantitative PCR revealed the expression of specific markers of SGEPs. Salivary gland-related genes: *CD24*, *LAMA1*, and *CHRM3* (A). Salivary gland secretion-related genes: *SLC9A1*, *SSC4D*, and *TRPV6* (B). Positive regulatory genes of inflammation: *F2R*, *KL*, and *BDKRB1* (C). Canonical Wnt pathway-related genes: *DKK1*, *SFRP5*, and *DLX5* (D). The data are presented as mean±SD and were normalized to β-actin in three independent experiments. The results are reported as the fold change compared to the wild-type human embryonic stem cells (hESCs) by unpaired, two-tailed Student's t-test; *$p<0.05$, **$p<0.01$, and ***$p<0.001$. WT-SGEPs: SGEPs derived from the wild-type hESCs, CF-SGEPs: SGEPs derived from cystic fibrosis transmembrane conductance regulator knockout hESCs.

qPCR data revealed that the mRNA expression level of *SFRP5* and *DLX5* was consistent with the trend of the RNA-Seq results of CF-SGEPs. There was no significant difference in the mRNA expression level of *DKK1* in CF-SGEPs compared with WT-SGEPs (Fig. 6D). These results suggest that CFTR protein may affect the Wnt pathway, which is also similar to other studies (27, 28). The aforementioned data suggest that CF-SGEPs share features highly associated with CF in terms of SG development, SG secretion and inflammation.

Discussion

To determine whether the hESCs-derived SGEPs, we constructed earlier are capable of modeling the SG development of patients with CF and could be used for development research, we first successfully constructed CFTR knockout hESCs. We have demonstrated that CFTR knockout hESCs have reduced CFTR protein expression and maintained pluripotency. We also observed that CF-SGEPs decreased the expression of CFTR protein. Furthermore, CF-SGEPs also simulated the disease characteristics of CF in terms of SG development and secretion.

Therefore, we used CRISPR-Cas9 technology to design a specific guide RNA on the *CFTR* gene and mutate the *CFTR* gene. After screening and sequencing, we generated CFTR knockout hESCs with a gene mutation; a base was inserted, and confirmed that the expression of CFTR protein was decreased. The phenotype of CF is that the mutation of CFTR leads to the defect of CFTR protein. In the process of protein processing and transportation to cell membrane, it is recognized and degraded by the endoplasmic reticulum, and the expression of CFTR protein is reduced (29). Most patients with CF have the ΔF508 mutation, which is characterized by no change in CFTR mRNA expression and decreased expression of mature CFTR protein. CFTR knockout hESCs showed no changes in mRNA levels (15). CFTR knockout hESCs showed no changes in mRNA levels in comparison to WT cells. Therefore, the CFTR knockout hESCs are similar to the characterization of the ΔF508 mutant. The results demonstrated that the CFTR knockout hESCs were successfully established, which provides a tool for studying CF. Moreover, CFTR knockout hESCs maintained the pluri-

potency of hESCs, indicating that the cells could be used to induce differentiation.

The CFTR knockout hESCs were induced SGEPs using our previously reported method (13). CFTR knockout hESCs formed fewer EBs than the WT and the expression of the ectoderm marker was decreased. Previous studies have demonstrated that SGs develop from ectoderm (11); therefore, a decrease in CFTR protein expression may affect the embryonic development of SGs. Importantly, the expression of CFTR protein in CF-SGEPs was decreased after 16 days of differentiation, consistent with the finding that SG in CF patients exhibited decreased expression of CFTR protein (30). Simultaneously, SGEPs derived from WT hESCs expressed CFTR protein. Studies have reported that CFTR protein was distributed in SGs (31), which demonstrated the specificity of the SGEP induction protocol we provided in the past. Previous studies have found that the expression of CFTR protein in mouse embryonic stem cells is decreased, which affects the expression of AXIN2 and CCND2, the target genes of the Wnt classic pathway, thereby affecting the development of mouse embryos (22). We also found that the expression of CCND1, CCND2 and LEF1in CF-SGEPs was reduced, indicating that the human CFTR protein may influence the canonical Wnt pathway.

Transcriptome analysis of CF-SGEPs and WT were performed and compared to each other further to investigate the correlation between CF-SGEPs and CF manifestation. RNA-Seq results revealed that CF-SGEPs exhibited many genes with reduced expression. LAMA1 contributes substantially to SG branching development (24). When LAMA1 is knocked down, the number of branches of SGs is decreased (25). We found that LAMA1 expression was also decreased in the reduced genes. The q-PCR results also showed this, so we speculated that the reduced expression of CFTR protein might affect the branching development of SGs, which is similar to the absence of granular ducts in SGs found in previous studies in CFTR knockout mice (20). CHRM3 is a SG-related marker (32). And the expression of CHRM3 in CF-SGEPs also was decreased. Previous studies have revealed that injection of CD24-positive cells or CD44-positive cells into SG injury models can help restore SG function (33). It has also been proposed that CD44 is involved in regulating the growth and renewal of normal SG tissue (34). We found that compared with WT-SGEPs, the expressions of CD24 and CD44 in CF-SGEPs decreased. In summary, the reduced expression of CFTR protein may influence the early development of SGs. The SGs of CF patients often exhibit insufficient salivary secretion, and decreased SG flow rate (18). The expression of SLC9A1 was decreased, the secretion of saliva decreased (35), and TRPV6 was also involved in the secretion of saliva (36). Interestingly, the expressions of SLC9A1 and TRPV6 were also decreased in CF-SGEPs, which was also similar to the SG characterization in CF patients. CF-SGEPs had decreased expression of the canonical Wnt pathway target gene *DLX5* and increased expression of the Wnt canonical pathway inhibitor SFRP5 (37), indicating that CFTR protein affects the canonical Wnt pathway. Previous studies have demonstrated that CF patients are susceptible to infection and develop an inflammatory response (26), which is also present in the SGs (38). We found that the CF-SGEPs had elevated expression of BDKRB1 and F2R, which are positively associated with inflammation (39, 40). In summary, the CF-SGEPs exhibited a strong association with the phenotype of CF patients. Furthermore, the differentiation of CF-SGEPs mimicked the development of SGs in CF patients.

In conclusion, we demonstrated that our previously reported protocol is capable of modeling the SG developmental disease through the differentiation of CFTR mutant hESCs into SGEPs, which could serve as models for studying the disease mechanism not only for CF but also for other development-related diseases of SGs, such as SG hypoplasia/hypoplasia, cleft lip, and palate syndrome.

ORCID

Shuang Yan, https://orcid.org/0009-0008-7297-5460
Yifei Zhang, https://orcid.org/0009-0006-9719-9782
Siqi Zhang, https://orcid.org/0009-0001-8540-0059
Shicheng Wei, https://orcid.org/0000-0001-6024-9615

Funding

This work was supported by Discipline Development Fund of School of Stomatology, Peking University.

Acknowledgments

We thank National Center for Protein Sciences at Peking University in Beijing, China, for assistance with providing Roche qPCR equipment and Nikon A1R confocal microscopy photography.

Potential Conflict of Interest

There is no potential conflict of interest to declare.

Availability of Data and Materials

The data used in this article will be available from the authors on reasonable request.

Code Availability

The RNA-Seq data files in this paper have been deposited into Gene Expression Omnibus (GEO). The accession number is GEO: GSE224547.

Authors' Contribution

Conceptualization: SY, SZ, SW. Data curation: SY, SZ, YZ. Formal analysis: SY, SZ, YZ. Funding acquisition: SW. Investigation: SY, SZ, YZ. Methodology: SY, SZ. Project administration: SY, SZ. Resources: SY, SZ, YZ. Validation: SZ, YS, YZ, SW. Writing – original draft: SY, SZ. Writing – review and editing: SZ, SY, YZ, SW.

Supplementary Materials

Supplementary data including three tables and three figures can be found with this article online at https://doi.org/10.15283/ijsc23036

References

1. Kolagar TA, Farzaneh M, Nikkar N, Khoshnam SE. Human pluripotent stem cells in neurodegenerative diseases: potentials, advances and limitations. Curr Stem Cell Res Ther 2020;15:102-110
2. Liu G, David BT, Trawczynski M, Fessler RG. Advances in pluripotent stem cells: history, mechanisms, technologies, and applications. Stem Cell Rev Rep 2020;16:3-32
3. Lancaster MA, Renner M, Martin CA, et al. Cerebral organoids model human brain development and microcephaly. Nature 2013;501:373-379
4. Drakhlis L, Devadas SB, Zweigerdt R. Generation of heart-forming organoids from human pluripotent stem cells. Nat Protoc 2021;16:5652-5672
5. McCracken KW, Catá EM, Crawford CM, et al. Modelling human development and disease in pluripotent stem-cell-derived gastric organoids. Nature 2014;516:400-404
6. Spence JR, Mayhew CN, Rankin SA, et al. Directed differentiation of human pluripotent stem cells into intestinal tissue in vitro. Nature 2011;470:105-109
7. Tam WL, Freitas Mendes L, Chen X, et al. Human pluripotent stem cell-derived cartilaginous organoids promote scaffold-free healing of critical size long bone defects. Stem Cell Res Ther 2021;12:513
8. Petersen MBK, Gonçalves CAC, Kim YH, Grapin-Botton A. Recapitulating and deciphering human pancreas development from human pluripotent stem cells in a dish. Curr Top Dev Biol 2018;129:143-190
9. Heslop JA, Duncan SA. The use of human pluripotent stem cells for modeling liver development and disease. Hepatology 2019;69:1306-1316
10. Emmerson E, Knox SM. Salivary gland stem cells: a review of development, regeneration and cancer. Genesis 2018;56:e23211
11. Holmberg KV, Hoffman MP. Anatomy, biogenesis and regeneration of salivary glands. Monogr Oral Sci 2014;24:1-13
12. Tanaka J, Senpuku H, Ogawa M, et al. Human induced pluripotent stem cell-derived salivary gland organoids model SARS-CoV-2 infection and replication. Nat Cell Biol 2022;24:1595-1605
13. Zhang S, Sui Y, Zhang Y, et al. Derivation of human salivary epithelial progenitors from pluripotent stem cells via activation of RA and Wnt signaling. Stem Cell Rev Rep 2023;19:430-442
14. Ooi CY, Durie PR. Cystic fibrosis from the gastroenterologist's perspective. Nat Rev Gastroenterol Hepatol 2016;13:175-185
15. Sermet-Gaudelus I, Vallée B, Urbin I, et al. Normal function of the cystic fibrosis conductance regulator protein can be associated with homozygous (Delta)F508 mutation. Pediatr Res 2002;52:628-635
16. Trapnell BC, Chu CS, Paakko PK, et al. Expression of the cystic fibrosis transmembrane conductance regulator gene in the respiratory tract of normal individuals and individuals with cystic fibrosis. Proc Natl Acad Sci U S A 1991;88:6565-6569
17. Barbero GJ, Sibinga MS. Enlargement of the submaxillary salivary glands in cystic fibrosis. Pediatrics 1962;29:788-793
18. da Silva Modesto KB, de Godói Simões JB, de Souza AF, et al. Salivary flow rate and biochemical composition analysis in stimulated whole saliva of children with cystic fibrosis. Arch Oral Biol 2015;60:1650-1654
19. El Khoury J, Haber E, Nasr M, Hokayem N. Botulinum neurotoxin A for parotid enlargement in cystic fibrosis: the first case report. J Oral Maxillofac Surg 2016;74:1771-1773
20. Nedvetsky PI, Emmerson E, Finley JK, et al. Parasympathetic innervation regulates tubulogenesis in the developing salivary gland. Dev Cell 2014;30:449-462
21. Ran FA, Hsu PD, Wright J, Agarwala V, Scott DA, Zhang F. Genome engineering using the CRISPR-Cas9 system. Nat Protoc 2013;8:2281-2308
22. Liu Z, Guo J, Wang Y, et al. CFTR-β-catenin interaction regulates mouse embryonic stem cell differentiation and embryonic development. Cell Death Differ 2017;24:98-110
23. Nanduri LS, Baanstra M, Faber H, et al. Purification and ex vivo expansion of fully functional salivary gland stem cells. Stem Cell Reports 2014;3:957-964
24. Kadoya Y, Nomizu M, Sorokin LM, Yamashina S, Yamada Y. Laminin alpha1 chain G domain peptide, RKRLQVQLSIRT, inhibits epithelial branching morphogenesis of cultured embryonic mouse submandibular gland. Dev Dyn 1998;212:394-402
25. Yang TL, Hsiao YC. Chitosan facilitates structure formation of the salivary gland by regulating the basement membrane components. Biomaterials 2015;66:29-40
26. Nichols DP, Chmiel JF. Inflammation and its genesis in cystic fibrosis. Pediatr Pulmonol 2015;50 Suppl 40:S39-S56
27. Sun H, Wang Y, Zhang J, et al. CFTR mutation enhances Dishevelled degradation and results in impairment of Wnt-

dependent hematopoiesis. Cell Death Dis 2018;9:275
28. Dumortier C, Danopoulos S, Velard F, Al Alam D. Bone cells differentiation: how CFTR mutations may rule the game of stem cells commitment? Front Cell Dev Biol 2021; 9:611921
29. Rowe SM, Miller S, Sorscher EJ. Cystic fibrosis. N Engl J Med 2005;352:1992-2001
30. Meng X, Clews J, Kargas V, Wang X, Ford RC. The cystic fibrosis transmembrane conductance regulator (CFTR) and its stability. Cell Mol Life Sci 2017;74:23-38
31. Zinn VZ, Khatri A, Mednieks MI, Hand AR. Localization of cystic fibrosis transmembrane conductance regulator signaling complexes in human salivary gland striated duct cells. Eur J Oral Sci 2015;123:140-148
32. Alshahran SA, Almufareh NA, Almarshady B, Alotaibi RK, Al-Qahtani WS. Effects of consuming *Catha edulis Forsk* (khat) on the gene manifestation of CHRM1 and CHRM3 in relation to salivary glands, saliva flow rates, pH and dental caries in Yemeni consumers. Open Dent J 2020;14:482-488
33. Jeong J, Baek H, Kim YJ, et al. Human salivary gland stem cells ameliorate hyposalivation of radiation-damaged rat salivary glands. Exp Mol Med 2013;45:e58
34. Fonseca I, Moura Nunes JF, Soares J. Expression of CD44 isoforms in normal salivary gland tissue: an immunohistochemical and ultrastructural study. Histochem Cell Biol 2000;114:483-488
35. Gonzalez-Begne M, Nakamoto T, Nguyen HV, Stewart AK, Alper SL, Melvin JE. Enhanced formation of a HCO3- transport metabolon in exocrine cells of Nhe1-/- mice. J Biol Chem 2007;282:35125-35132
36. Shen ZJ, Han YC, Nie MW, Xiang RL, Xie HZ. Analyses of circRNA and mRNA profiles in the submandibular gland in hypertension. Genomics 2021;113(1 Pt 1):57-65
37. Zou DP, Chen YM, Zhang LZ, et al. SFRP5 inhibits melanin synthesis of melanocytes in vitiligo by suppressing the Wnt/β-catenin signaling. Genes Dis 2020;8:677-688
38. Harutyunyan SA, Simonyan KG, Mkrtchyan NM, Kashirskaya NY, Libik M, Macek M. [Sialadenitis in cystic fibrosis: case report]. Doctor.Ru 2020;19:66-68 Russian
39. Bachvarov DR, Hess JF, Menke JG, Larrivée JF, Marceau F. Structure and genomic organization of the human B1 receptor gene for kinins (BDKRB1). Genomics 1996;33:374-381
40. Lv J, Liu J, Chao G, Zhang S. PARs in the inflammation-cancer transformation of CRC. Clin Transl Oncol 2023;25:1242-1251